

Araştırma Makalesi / Research Article**Evaluation of Mechanical Properties of PLA Auxetic Structures Produced by Additive Manufacturing**Ahu ÇELEBİ^{1*}, Mustafa Mertcan İMANÇ²

¹ Manisa Celal Bayar Üniversitesi, Mühendislik Fakültesi, Metalurji ve Malzeme Mühendisliği Bölümü, Manisa, Türkiye,
ORCID ID: <https://orcid.org/0000-0003-0401-5384>, ahu.celebi@cbu.edu.tr

² Manisa Celal Bayar Üniversitesi, Mühendislik Fakültesi, Metalurji ve Malzeme Mühendisliği Bölümü, Manisa, Türkiye,
ORCID ID: <https://orcid.org/0009-0004-7999-2096>, mertcanimanc@icloud.com

Geliş/ Received: 05.06.2023;**Kabul / Accepted:** 08.08.2023

ABSTRACT: FDM (fused deposition modeling) is one of the most commonly used technologies in additive manufacturing. This technology is used to additively manufacture components from various polymer materials, mostly PLA (polylactic acid), etc. PLA filament is a widely used polymer for 3D printing due to its biodegradability, biocompatibility, and processability. In the study, PLA raw material and cellular auxetic structures were used in the design. Auxetic designs are called metamaterials, they are structures with advanced properties and can be obtained with various geometries. The auxetic designs used in the study are missing rib, re-entrant honeycomb and chiral. One of the biggest advantages of auxetic cellular materials is that it is not bulk material. Having a skeletal structure provides high strength at low density. Today, based on this mechanism, designs that can be used in engineering applications are being studied. It has an important place especially in the medical field, as well as in the areas where high precision and specific products are designed and produced. Considering its relationship with 3D printing technology, 3D printing enables the fabrication of auxetic structures for complex and personal designs. The novelty of auxetic structures comes from their topological features, which display counterintuitive response to the applied load. For the purpose of compare the properties of mechanical tensile, compression, surface roughness tests were applied. It is concluded that the presence of chiral structures improves mechanical performance. The chiral auxetic sample exhibited a maximum stress of 6.68 MPa, the missing-rib auxetic sample displayed a maximum stress of 2.26 MPa, and the re-entrant auxetic sample demonstrated a maximum stress of 3.68 MPa. These results obtained from the tests align well with the range reported in the literature, which falls between 1-12 MPa. The surface roughness of the all-auxetic structure, perpendicular to the printing direction was higher than the measurements taken parallel to the printing direction.

Keywords: Additive Manufacturing, Fused Deposition Modeling, Auxetic design, PLA, Mechanical properties

*Sorumlu yazar / Corresponding author: ahu.celebi@cbu.edu.tr

Bu makaleye atıf yapmak için / To cite this article

Çelebi, A., İmanç, M.M. (2023). Evaluation of Mechanical Properties of PLA Auxetic Structures Produced by Additive Manufacturing. Journal of Materials and Mechatronics: A (JournalMM), 4(2), 384-396.

1. INTRODUCTION

The greater part of engineering materials exhibit a positive Poisson's ratio, but there are only a few materials that possess a negative Poisson's ratio. These materials are often called as auxetic materials (Anurag, 2010; Alderson, A. and Alderson, K.L, 2007; Baughman et al., 1998). The term auxetic is of Greek origin and comes from auxetikos and the meaning of the word tends to be extended. It was first used by Professor Ken Evans in 1991 (Evans, 1991). Unlike materials with positive Poisson's ratio, auxetic materials expand as they are stretched and contract as they are pressed, an extraordinary property, as shown in Figure 1. (Luo, 2022). Although this feature has been known since the last century, its understanding as mechanics and logic and its application to materials started in the 1980s. For the first time, “foam” structures with negative Poisson ratio were published in Science by Rod Lakes in 1987 (Lakes, 1987).

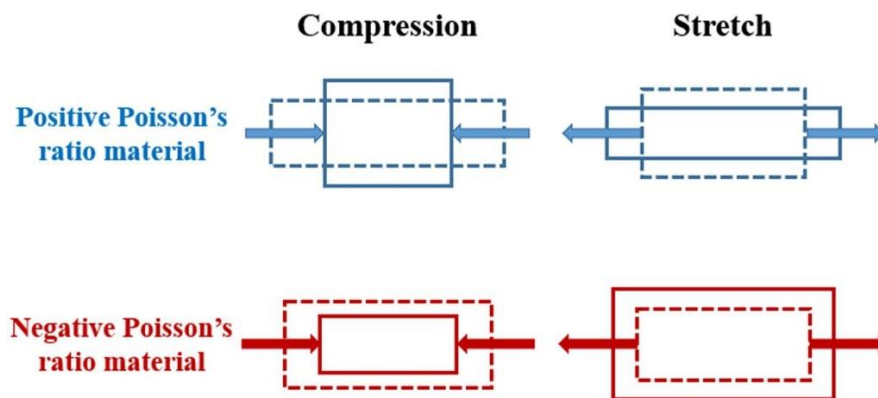


Figure 1. Deformation of conventional and auxetic materials (Luo, 2022)

Auxetic materials show an unusual feature by thickening when pulled, and there are some properties unique to these materials. This unique property makes them highly desirable for various industrial and biomedical applications. Auxetic materials are used in applications such as protective gear, smart textiles, impact-resistant materials, and tissue engineering (Joseph et al., 2021). Auxetic materials have a variety of distinct characteristics that render them extremely desirable in various applications. These characteristics include:

- Negative Poisson's ratio: Auxetic materials exhibit lateral expansion when subjected to stretching, making them highly effective in impact-resistant materials.
- High energy absorption: Auxetic materials can absorb high amounts of energy when subjected to impact, making them ideal for use in protective gear.
- High flexibility: Auxetic materials are highly flexible, making them ideal for use in smart textiles and wearable technologies.
- Biocompatibility: Auxetic materials are biocompatible, making them ideal for use in tissue engineering and medical implants.

Auxetic materials possess exceptional mechanical characteristics such as enhanced resistance to indentation, shear, fracture, and efficient energy absorption. Nonetheless, the stiffness of auxetic structures is generally lower than that of solid materials due to the presence of voids. Auxetic materials are used in various industrial and biomedical applications, including:

- Protective gear: Auxetic materials are used in applications such as body armor and helmets to absorb high amounts of energy during impacts.
- Smart textiles: Auxetic materials are used in smart textiles and wearable technologies to provide high flexibility and improved comfort.

- Impact-resistant materials: Auxetic materials are used in applications such as impact-resistant materials and cushioning.
- Tissue engineering: Auxetic materials are used in tissue engineering and medical implants due to their biocompatibility and flexibility (Mir et al., 2014; Dirrenberger et al., 2012; Liu et al., 2010).

Various methods have been searched and refined to achieve auxetic structures, aiming to create flexible, cost-effective, and time-saving processes. The production of auxetic structures typically involves modifications to foaming techniques and the combination of conventional processes like compression, heating, and cooling. Over time, several enhancements have been explored within this manufacturing process, including alterations to the mold's geometry or the use of pins for fabricating larger samples (Duncan et al., 2016). However, additive manufacturing can be a valuable solution to overcome these limitations, as it allows for the design of complex geometric structures in a cost-effective and rapid manner, even on a significant scale. Thus, additive manufacturing methods are currently intensively researched to produce components from various structural materials, i.e. superalloys, Al-alloys and stainless steels, in the industry (Çam, 2022; Günen et al, 2023a; Günen et al, 2023b; Ceritbinmez et al, 2023). The progress of additive fabrication has currently achieved a degree of adaptability that enables the creation and fine-tuning of architectures possessing an adverse Poisson's ratio and multifunctional capacities (Joseph et al., 2021). Among the various additive manufacturing techniques available, the optimal and flexible approach is the FDM process, which enables the manufacturing of polymer materials with negative Poisson ratios and various pattern types (Carton et al., 2019). FDM, as a unique material extrusion technique, offers several advantages in the realm of additive manufacturing. It enables the customization of personalized items, encourages design flexibility, and simplifies the production of complex elements for intricate parts, thereby minimizing expenses and lead times in product development. Additionally, FDM boasts other significant benefits, such as inexpensive and low-maintenance machines, as well as cost-effective stock materials compared to other additive manufacturing techniques. Moreover, it presents opportunities for modifying component characteristics and advancing materials inspired by nature's structures (Mocerino et al., 2023).

2. GEOMETRIC MODELLING

Depending on the required load and geometry, various topologies can be realized, as highlighted in Figure 2 (Liu et al., 2010). Numerous studies have examined different structures using various auxetic models, which can be categorized as re-entrant structures, rotating deformation models, and chiral structures (Guo, Y. et al., 2020; Duncan et al., 2016; Carneiro et al., 2013; Alderson, A 2007).

Re-entrant structures exhibit auxetic behavior by flexing diagonal ribs, resulting in an outward unfold under tension. This deformation mechanism provides the structure with its auxetic properties. On the other hand, rotating models consist of complex systems with rigid geometries (Alderson, A. and Alderson, K.L, 2007). Auxetic structures prove to be beneficial when specific mechanical properties need improvement. For instance, chiral structures demonstrate increased resistance to global and local buckling compared to conventional honeycomb structures (Miller et al., 2010; Spadoni et al., 2005). Negative Poisson ratio foams, on the other hand, exhibit higher energy absorption in dynamic impacts compared to conventional foams, resulting in improved stiffness (up to 4 times), indentation stiffness (up to 1.4 times), and energy absorption (up to 3 times) (Li et al., 2020; Lakes R.S. and Elms, K., 1993). They also exhibit enhanced indentation resilience and

hardness, increasing threefold compared to conventional materials under low-load conditions (Alderson et al., 2000; Chan, N. and Evans, K.E., 1998). Fracture toughness can experience an increase of up to 225% (Choi, J.B. and Lakes, R.S., 1996; Yang et al., 2017). The auxetic effect is further enhanced beyond the yield point (Dirrenberger et al., 2012).

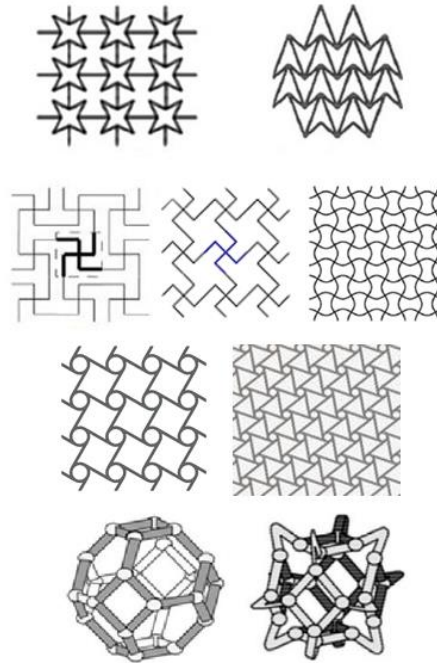


Figure 2. Different kind of auxetic topology reproduced from SAGE journals (Wang et al., 2001)

Moreover, the emergence of novel additive manufacturing (AM) techniques offers the potential to fabricate intricate shapes with fascinating mechanical properties, as well as multifunctional and smart attributes (Joseph et al., 2021). However, to fully exploit these opportunities, significant efforts are needed to address the existing processing challenges. Overcoming these technological limitations and developing scalable techniques for the production of auxetic structures with customized microstructures and properties, while transitioning from small-scale prototypes to industrial-grade products, requires substantial dedication and research.

In project, where we aim to achieve optimum performance from materials by altering the topology. Considering this literature, we decided to used in the study are missing rib, re-entrant honeycomb and chiral with the auxetic designs. For the purpose of compare the mechanical properties of the manufactured parts, mechanical tensile, compression, hardness and surface roughness tests were applied.

3. MATERIALS AND METHODS

3.1 Design of Auxetic Structure

Different programs are used to create designs for 3D printers. It is possible to create geometric designs with the CAD program, which is one of them. After the model is created, the file can be exported in formats that 3D printing programs can use. After the 3D model has been created, the Cura program is available for editing the necessary parameters for the printing process, separating them into layers and previewing the model. The Cura program to be used in the study is a software developed by Ultimaker, a leading 3D printer manufacturer. In this program, the layers required in

that the dimensions and cell orientations of the unit cells in the tensile and compression test samples were the same. Surface area values calculated automatically through the drawing program are given in the Table 1.

Table 1. The surface area and weight values according to auxetic structure

Auxetic structure type	Surface area (mm ²)	Weight (gr)		
Chiral Auxetic Structure (Tensile Sample)	1636	6.37	6.35	6.36
Missing-rib Auxetic Structure (Tensile Sample)	1650	6.06	6.05	6.07
Re-entrant Auxetic Structure (Tensile Sample)	1650	5.86	5.88	5.89

3.2 Preparation of Sample

PLA, one of the most common polymers used in additive manufacturing methods, is an eco-friendly biopolymer and thermoplastic derived from corn starch and sugar cane, thus posing no risks to human health (Çelebi, 2022). This feature has made PLA widely used in the biomedical field. In addition, PLA is a biodegradable material and it can decompose in less than three months. Automotive, aerospace, biomedical, and robotics fields can be shown as the most extensive usage areas of PLA polymer (Taşdemir, 2022).

The structures for which the auxetic designs were created were printed by 3D FDM technology device using PLA filament raw material. The designs of the test samples were converted to STL file format and opened in the slicer program, and the models positioned on the virtual production table were sliced in layers with the Ultimaker Cura 4.4.1 program and became ready for production after the optimum manufacturing parameters were entered. The manufacturing parameters used are given in Table 2.

Table 2. The manufacturing parameters used in our study

Printer Type	Anycubic i3 Mega S
Filament type	PLA
Nozzle temprature	200 C
Build Platform temprature	65 C
Infill	% 100
Nozzle diameter	0,4 mm
Layer thickness	0,2 mm
Print speed	60mm/s
Print time (for tensile test)	32 dk

3.3 Tensile Test

Figure 6 depicts the complete auxetic tensile specimens. An AUTOGRAPH – AG-IS 100KN tensile strength machine was employed for conducting the experiments. Specimens are placed in the grips of the universal tester at a specified grip separation and pulled until failure. For ISO 527 the test speed is typically 5 or 50mm/min for measuring strength and elongation and 1mm/min for measuring modulus. The specimens were securely positioned between the lower and upper grips of the tensile apparatus and underwent a pulling procedure at a rate of 5.00 mm per minute according to ISO 527 standard. The tests were carried out at ambient temperature at room temperature and an average of 50% humidity. The performed examinations encompassed the evaluation of tensile potency, tensile elongation, and percentage elongation measurements for the specimens.

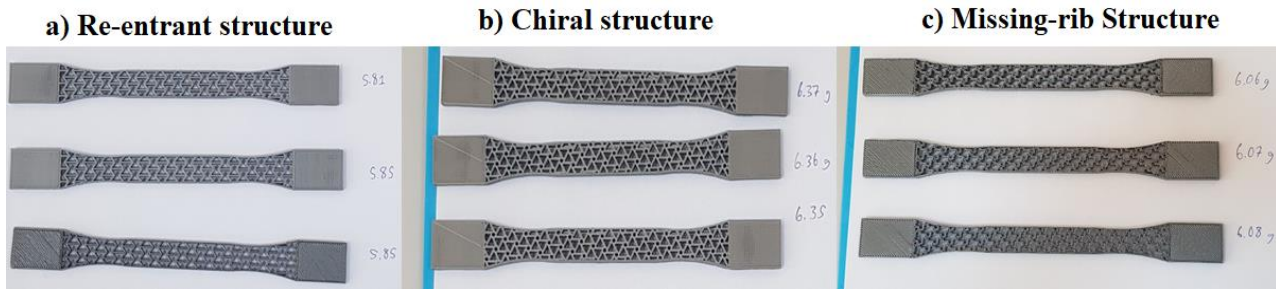


Figure 6. Tensile specimens a. Re-entrant b. Chiral c. Missing-rib auxetic structure

3.4 Compression Test

The fundamental aim of compression testing is to ascertain the characteristics and reaction of a material when exposed to a compressive load, through the measurement of essential parameters like stress and strain. The elastic modulus between the compressive force applied to pertaining to the material and the compressive resilience, yield resilience, ultimate resilience, elastic threshold, and other parameters of the material is determined. By comprehending these distinct variables and the corresponding values related to a specific material, it becomes evident whether the material is appropriate for specific applications or prone to failure under particular stress conditions. Uniaxial compression experiments were conducted utilizing a universal testing machine, AUTOGRAPH – AG-IS, with a measurement range of 10 kN and a precision of 0.001 N. The complete auxetic compression specimens are illustrated in Figure 7.

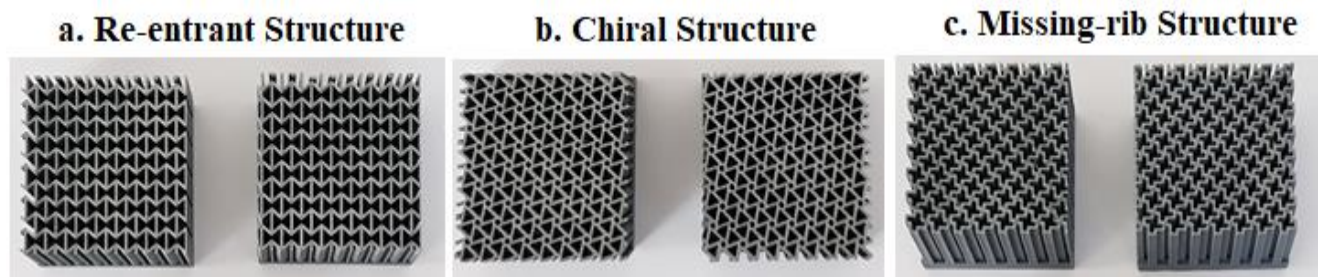


Figure 7. Compression specimens a. Re-entrant b. Chiral c. Missing-rib auxetic structure

3.5 Surface Roughness

The surface roughness of AM parts is typically measured with a profilometer to achieve an arithmetical mean of height of a line (Ra). However, the surface structure is dependent on the overlap of hatches and hatch strategy. Accurate quantitative analysis of surface roughness is therefore essential to qualify the functionality and appearance of a surface. and is thus important to quantify accurately. The direct measurement method with the device is the quantitative analysis method. In this method, a point-contact adapter is used and the surface roughness is determined numerically. The point-contact adapter moves over the surface of the part and the printouts are read on the device as an indicator. The principle is that the fine-tipped probe or point-contact adapter moves on the surface of the finished part. Vertical movements of the point-contact adapter due to surface irregularities are used to evaluate the roughness. The tip of the point-contact adapter is made of a diamond or similar hard material. As a result of the movement of the point-contact adapter, electrical signals are generated and these electrical signals are used as output. The standard for measuring surface roughness is TS EN ISO 21920-2: 2022. The roughness profile cutoff value (λ_c) is 0,8 mm and drive unit speed is 0,5 mm/s.

Taking into account the layer-by-layer forming process, each sample contains two sides with different surface roughness, and each side has two different surface roughness. 3 measurements perpendicular to the printing direction and 3 measurements parallel to the printing direction (Fig 8) were taken from each surface (bottom surface and upper surface) of the samples produced with using a 3D printer with SJ-210 Mitutoyo roughness tester and the Ra data obtained were compared.

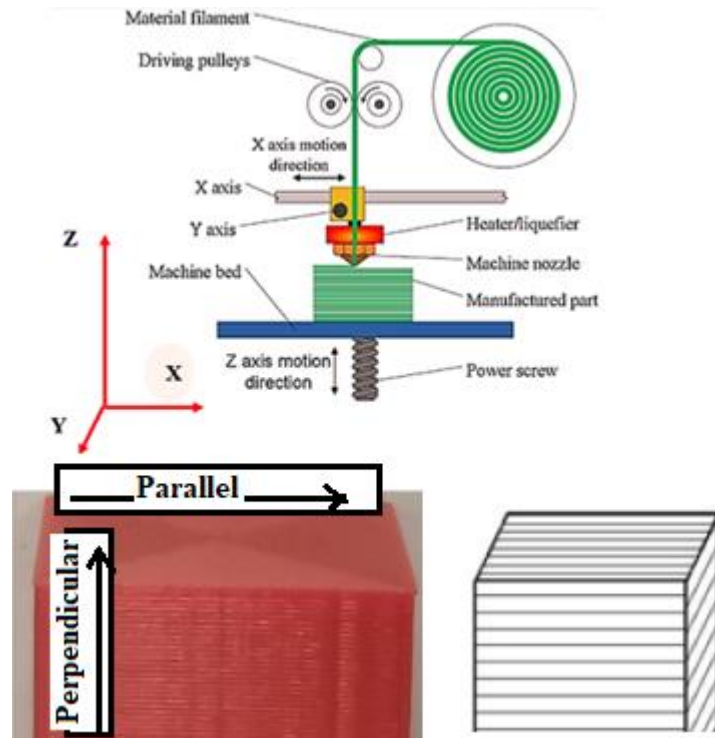


Figure 8. Measurements of Perpendicular and Parallel to the printing direction

4. RESULTS AND DISCUSSION

4.1 Tensile Test

Stress-displacement values were calculated based on the load-displacement data obtained from the Universal Testing Machine (UTM). For maximum stress (σ -N/mm²), a total of 9 measurements were made for 3 different auxetic structures with three replicates. From Table 3 it can be seen that all of the experimentally determined values for the mechanical properties in different auxetic structures. Figure 9 illustrates the stress-displacement relationship of the tensile specimens fabricated with three distinct auxetic structures, as discussed in section 3.1. The presence of the auxetic structure had a significant impact on the overall performance of the specimens. The chiral auxetic sample exhibited a maximum stress of 6.68 MPa, the missing-rib auxetic sample displayed a maximum stress of 2.26 MPa, and the re-entrant auxetic sample demonstrated a maximum stress of 3.68 MPa. These results obtained from the tests align well with the range reported in the literature, which falls between 1-12 MPa (Berkay Ergene).

Table 3. Tensile testing values according to auxetic structure

Auxetic structure type	Maximum Stress (σ -N/mm ²)	Maximum Strain (%)	Maximum Displacement (mm)
Chiral	6.68	1.228	0.243
Auxetic Structure	6.48	1.103	0.225
Missing-rib	6.38	0.985	0.290
Missing-rib Auxetic Structure	2.26	0.654	-
Re-entrant	2.07	0.510	0.235
Auxetic Structure	1.69	0.647	0,225
Re-entrant Auxetic Structure	2.92	0.958	0.212
	3.15	0.766	0.370
	3.68	1.109	0.264

The walls within each distinct auxetic structure experienced failure, thereby reducing the load-carrying capacity of the structure. With further loading, the remaining auxetic cells fractured due to the conversion of the applied tensile load into shear load. In addition, it is seen that the re-entrant auxetic design has a strength between the two, while the missing rib auxetic structure has the lowest strength value.

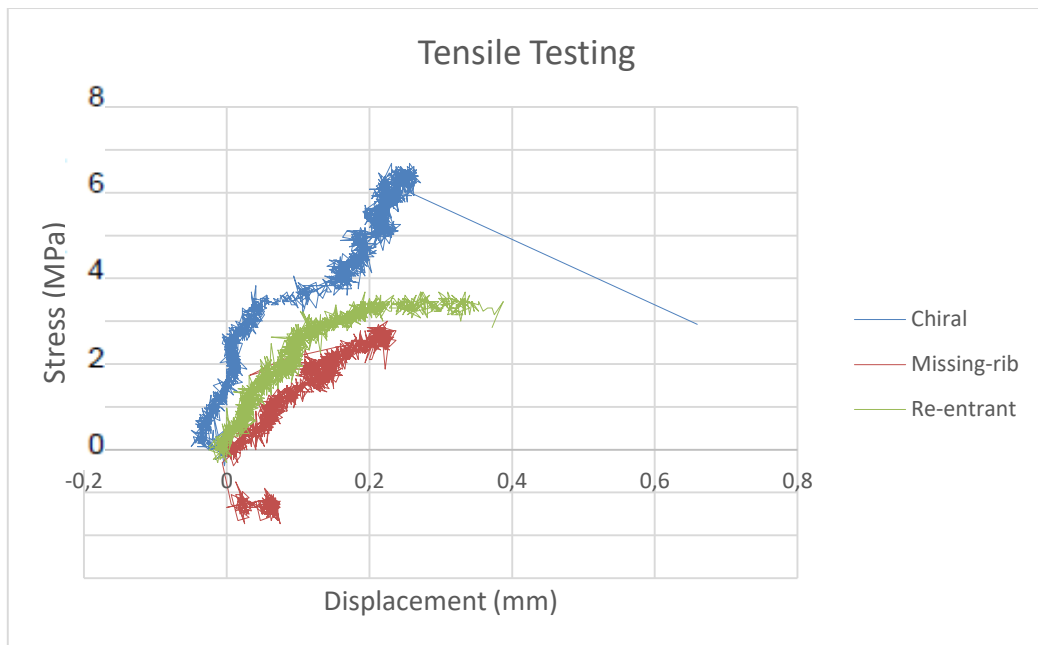


Figure 9. Stress-displacement curve of tensile samples

4.2 Compression Test

Stress-displacement obtained as a result of the compression test of all auxetic structures curves are presented in Figure 10. Compression test was repeated 3 times. As shown in Figure 10, the chiral auxetic structure has the highest compressive strength as the value in auxetic materials. The lowest compression value to failure was achieved with a re-entrant pattern in auxetic structures. However, the highest displacement value was achieved with a missing-rib pattern in auxetic structures which is the compression value between chiral and re-entrant auxetic.

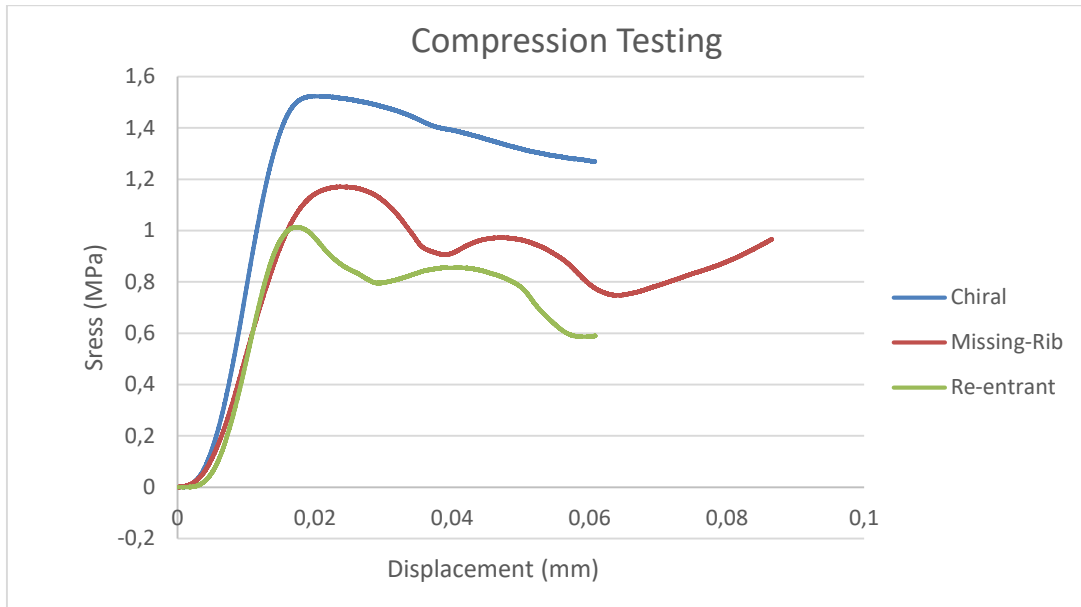


Figure 10. Outcomes obtained from compression test of 3 different auxetic structures

4.3 Surface Roughness

The surface roughness values of each auxetic design printed as a result of the studies, both parallel and perpendicular to the printing direction, are given in the Table 4. As a result of the comparisons, it was observed that the measurements taken perpendicular to the printing direction were higher than the measurements taken parallel to the printing direction. During the experiment, the surface treatment range was set as 4.60 mm.

Table 4. Surface roughness values according to printing direction

Auxetic structure type	Parallel to printing direction Ra (µm)	Perpendicular to printing direction Ra (µm)
Chiral Auxetic Structure	4.225	8.620
Missing-rib Auxetic Structure	4.328	7.327
Re-entrant Auxetic Structure	4.447	7.689
Chiral Auxetic Structure	7.573	9.097
Missing-rib Auxetic Structure	7.120	8.616
Re-entrant Auxetic Structure	7.290	8.956
Chiral Auxetic Structure	3.886	8.924
Missing-rib Auxetic Structure	4.251	7.849
Re-entrant Auxetic Structure	4.025	7.984

5. CONCLUSION

In this work, three types of auxetic structures were compared according to tensile, compression and surface roughness result. In order to make a correct comparison between different topologies, the specimen densities were kept close to each other for the three different geometries. The following conclusions can be drawn:

- It is concluded that the presence of chiral structures improves mechanical performance. The chiral structure exhibited larger stress than other auxetic structures.
- The chiral auxetic sample exhibited a maximum stress of 6.68 MPa, the missing-rib auxetic sample displayed a maximum stress of 2.26 MPa, and the re-entrant auxetic sample demonstrated a maximum stress of 3.68 MPa. These results obtained from the tests align well with the range reported in the literature, which falls between 1-12 Mpa.
- The surface roughness of the all-auxetic structure, perpendicular to the printing direction was higher than the measurements taken parallel to the printing direction.

In project, where we aim to achieve optimum performance from materials by altering the topology, the tensile test revealed that the missingrib geometry exhibited the lowest performance. However, when the average of the maximum tensile stresses measured from three repeated tests was calculated, it was observed that the reentrant structure achieved approximately 60% higher pre-rupture maximum stress values compared to missingrib, while the chiral structure exhibited approximately 100% higher values. According to the compression test results, the reentrant structure exhibited the lowest performance, while the missingrib structure achieved approximately 20% higher maximum force values and the chiral structure reached approximately 40% higher maximum force values. In the compression test graph, the area under the graph, obtained by taking displacement data on the x-axis, provides a clue about the amount of energy absorption of the materials, and it is observed to be parallel to the performance values in the compression test.

The results provide new ideas for the design of novel metamaterials with superior mechanical properties in the future. However, it is also worth further research to design three-dimensional metamaterials based on unit cells with variable strength, such as variable structures. These auxetic metamaterials with different geometrical configurations could expand potential applications of auxetics in civil, medical and protective engineering.

This study indicates that the chiral structure is a promising energy absorbing structure subjected to quasi-static loading. However, in some applications, auxetic structures may be subjected to dynamic loading. Therefore, it will be interesting to examine the mechanical performance of the chiral structure under dynamic loading conditions. The auxetic cellular materials and structures show huge potential to become important light-weight structural materials of the future with further development of additive manufacturing technologies or with introduction of some new, more cost-effective manufacturing techniques.

6. CONFLICT OF INTEREST

Author(s) approve that to the best of their knowledge, there is not any conflict of interest or common interest with an institution/organization or a person that may affect the review process of the paper.

7. AUTHOR CONTRIBUTION

Ahu ÇELEBİ contributed determining the concept of the research and research management, Ahu ÇELEBİ and Mustafa Mertcan IMANÇ contributed design process of the research and research management, data analysis and interpretation of the results, critical analysis of the intellectual content, preparation of the manuscript, and final approval and full responsibility.

8. REFERENCES

- Alderson, A.; Alderson, K.L. Auxetic materials. *Proc. Inst. Mech. Eng. Part G J. Aerosp. Eng.* 221, 565–575, 2007.
- Alderson, K.L.; Fitzgerald, A.; Evans, K.E. The strain dependent indentation resilience of auxetic microporous polyethylene. *J. Mater. Sci.*, 35, 4039–4047, 2000.
- Anurag, C. K. Anvesh, and S. Katam, “Auxetic materials,” *Int. J. Research in Appl. Sci. Eng. Technol.*, 3, (4), 1176–1183, 2015.
- Baughman, R.H.; Shacklette, J.M.; Zakhidov, A.A.; Stafström, S., Negative poisson’s ratios as a common feature of cubic metals. *Nature* 1998, 392, 362–365. [CrossRef]
- Çam G., Prospects of producing aluminum parts by wire arc additive manufacturing (WAAM), *Materials Today: Proceedings*, 62 (1), 77-85, 2022.
- Carneiro, V.H.; Meireles, J.; Puga, H. Auxetic materials—A review. *Mater. Sci.* 31, 561–571, 2013.
- Carton, M.A.; Ganter, M. Fast and simple printing of graded auxetic structures. In *Proceedings of the 30th International Solid Freeform Fabrication—An Additive Manufacturing Conference SFF*, University of Texas: Austin, TX, USA; pp. 2270–2279, 2019.
- Çelebi, A., Experimental and statistical investigation of the bending and surface roughness properties on three-dimensional printing parts. *Journal of Testing and Evaluation* 50, no. 4, 2069–2082, 2022.
- Ceritbinmez F., Günen A., Gürol U., Çam G., A comparative study on drillability of Inconel 625 alloy fabricated by wire arc additive manufacturing, *Journal of Manufacturing Processes*, 89, 150-169, 2023.
- Chan, N.; Evans, K.E. Indentation resilience of conventional and auxetic foams. *J. Cell. Plast.* 34, 231–260, 1998.
- Choi, J.B.; Lakes, R.S. Fracture toughness of re-entrant foam materials with a negative Poisson’s ratio: Experiment and analysis. *Int. J. Fract.* 80, 73–83, 1996.
- Dirrenberger, J.; Forest, S.; Jeulin, D. Elastoplasticity of auxetic materials. *Comput. Mater. Sci.* 64, 57–61, 2012.
- Duncan, O.; Foster, L.; Senior, T.; Allen, T.; Alderson, A. A comparison of novel and conventional fabrication methods for auxetic foams for sports safety applications. *Procedia Eng.* 147, 384–389, 2016.
- Ergene, B., Yalçın B., Eriyik yığma modelleme (EYM) ile üretilen çeşitli hücreli yapıların mekanik performanslarının incelenmesi, *Journal of the Faculty of Engineering and Architecture of Gazi University* 38:1, 201-217, 2023.
- Evans K.E., Nkansah M.A., Hutchison I.J., Rogers S.C., Molecular Network Design, *Nature* 353, 124, 1991.
- Günen A., Gürol U., Koçak M., Çam G., A new approach to improve some properties of wire arc additively manufactured stainless steel components: Simultaneous homogenization and boriding, *Surface & Coating Technology*, 460, 129395, 2023b.
- Günen A., Gürol U., Koçak M., Çam G., Investigation into the influence of boronizing on the wear behavior of additively manufactured Inconel 625 alloy at elevated temperature, *Progress in Additive Manufacturing*, 2023a.
- Guo, Y.; Zhang, J.; Chen, L.; Du, B.; Liu, H.; Chen, L.; Li, W.; Liu, Y. Deformation behaviors and energy absorption of auxetic lattice cylindrical structures under axial crushing load. *Aerosp. Sci. Technol.* 98, 105662, 2020.

- Hui Chen Luo, Xin Ren, Yi Zhang, Xiang Yu Zhang, Xue Gang Zhang, Chen Luo, Xian Cheng, Yi Min Xie, Mechanical properties of foam-filled hexagonal and re-entrant honeycombs under uniaxial compression, *Composite Structures*, Volume 280, 2022,
- Joseph, A.; Mahesh, V.; Harursampath, D. On the application of additive manufacturing methods for auxetic structures: A review. *Adv. Manuf.* 9, 342–368, 2021.
- Lakes R.S., Foam structures with a negative Poisson's ratio” *Science*, 235:1038–1040, 1997.
- Lakes, R.S.; Elms, K. Indentability of conventional and negative poisson’s ratio foams. *J. Compos. Mater.* 27, 1193–1202, 1993.
- Li, T.; Liu, F.; Wang, L. Enhancing indentation and impact resistance in auxetic composite materials. *Compos. Part B Eng.* 198, 108229, 2020.
- Liu, Y.; Hu, H. A review on auxetic structures and polymeric materials. *Sci. Res. Essay*, 5, 1052–1063, 2010.
- Miller, W.; Smith, C.W.; Scarpa, F.; Evans, K.E. Flatwise buckling optimization of hexachiral and tetrachiral honeycombs. *Compos. Sci. Technol.* 70, 1049–1056, 2010.
- Mir, M.; Ali, M.N.; Sami, J.; Ansari, U. Review of mechanics and applications of auxetic structures. *Adv. Mater. Sci. Eng.* 1–17, 2014.
- Mocerino, D.; Ricciardi, M.R.; Antonucci, V.; Papa, I. Fused deposition modelling of polymeric auxetic structures: A Review. *Polymers*. 15, 1008, 2023.
- Spadoni, A.; Ruzzene, M.; Scarpa, F. Global and local linear buckling behavior of a chiral cellular structure. *Phys. Status Solidi.* 242, 695–709, 2005.
- Taşdemir M., Experimental and numerical investigation of mechanical properties of additively manufactured auxetic structures, Master Thesis of Middle East Technical University, Turkey, 2022.
- Wang, Y.-C.; Lakes, R.; Butenhoff, A. Influence of cell size on re-entrant transformation of negative poisson’s ratio reticulated polyurethane foams. *Cell. Polym.* 20, 373–385, 2001.
- Yang, S.; Chalivendra, V.B.; Kim, Y.K. Fracture and impact characterization of novel auxetic Kevlar®/Epoxy laminated composites. *Compos. Struct.* 168, 120–129, 2017.